Transportation Research Interdisciplinary Perspectives 18 (2023) 100766

Contents lists available at ScienceDirect

Transportation Research Interdisciplinary Perspectives

journal homepage: www.sciencedirect.com/journal/transportation-research-interdisciplinary-perspectives

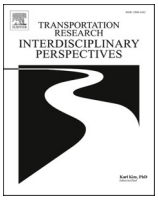

Snow coverage estimation using camera data for automated driving applications

Nicholas A. Goberville [a], Kyle R. Prins [a], Parth Kadav [a], Curtis L. Walker [b], Amanda R. Siems-Anderson [c], Zachary D. Asher [a]

[a] Energy Efficient & Autonomous Vehicles Lab, Dept. of Mechanical & Aerospace Engineering, Western Michigan University, Kalamazoo, MI 49008, United States
[b] Weather Systems and Assessment Program, Research Applications Laboratory, National Center for Atmospheric Research, Boulder, CO 80305, United States
[c] Surface Transportation Weather, Research Applications Laboratory, National Center for Atmospheric Research, Boulder, CO 80305, United States

ARTICLE INFO

Keywords:
ADAS (Advanced Driver Assistance Systems)
ML (Machine Learning)
ODD (Operational Design Domain)
NCEI (National Center for Environmental Information)

ABSTRACT

In the U.S., over 38,000 fatalities occur every year due to automotive accidents where 24% of these accidents are attributable to inclement weather. Automated driving systems have shown to decrease up to 21% of potential collisions, however, these systems do not operate in inclement weather. The camera's reliance on clear lane line detections cease the functionality of the safety systems when occlusions occur due to precipitation. For these systems to become operational during conditions such as snow coverage, therefore leading to a greater impact on safety, new research and development is needed to focus on inclement weather scenarios. This study addresses this need by first collecting a new dataset consisting of raw camera images along arterial roads in Kalamazoo, MI and additionally collecting snow precipitation data from the National Center for Environmental Information. With this data, snow coverage estimation models were developed to automatically determine categories of snow coverage. The models were developed by investigating various machine learning algorithm types, image predictors, and the presence of snow precipitation data. The final model resulted in 95.63% accuracy for categorizing the instance as either none, standard, or heavy snow coverage. These categories are important for future development of purpose-build algorithms that identify drivable regions in various levels of snow coverage for future automated driving systems. The results demonstrate that snow estimation is a near-term achievable task and that the presence weather data improves accuracy. With the addition of snow-coverage estimation, automated driving systems can be developed to react to these different conditions respectively and further reduce the nearly 6,000 annual fatalities caused driving in adverse weather.

1. Introduction

Automated driving systems such as Advanced Driver Assistance Systems (ADAS) are being implemented at an exponential rate in automotive passenger vehicles due to rapidly evolving computers, sensors, and algorithms. To date, ADAS products in the U.S. have been successful because they have directly reduced the number of front-to-rear collisions by 50%, sideswiping collisions by 11%, and lane-change crashes by 21% (Insurance Institute for Highway Safety, 2020). As this technology evolves, ADAS products will eventually transition into level 5 Autonomous Driving Systems (ADS) to further improve these accident reduction metrics (Society of Automotive Engineers, 2021). However, a major unsolved hurdle for widespread realization of level 5 ADS is the limitation of the weather operational design domain (ODD). Current ADAS technologies are only operational during ideal conditions, i.e. highway driving in clear weather (Thorn and Kimmel, 2018; National and Traffic Safety Administration, 2018; Flannagan et al., 2016; European New Car Assessment Program, 2019; Neumeister et al., 2019). Therefore, to improve the efficacy of ADAS and eventually ADS products in reducing accidents and fatalities, the ODD must be expanded to include adverse weather conditions (Walker et al., 2020).

An example of a general ADAS product system is shown in Fig. 1 where adverse weather specifically challenges the perception subsystem. In general, the perception system is responsible for constructing the real-time interpretation of the vehicle's operating environment using sensors such as camera, LiDAR, and radar. Each sensor provides unique benefits for perception but results in different error sources from weather (Goberville et al., 2020; Vargas et al., 2021). Cameras, specifically, are the most susceptible to occlusions of lane markings caused by

E-mail addresses: nickgoberville21@gmail.com (N.A. Goberville), kyle.r.prins@wmich.edu (K.R. Prins), parth.kadav@wmich.edu (P. Kadav), walker@ucar.edu (C.L. Walker), aander@ucar.edu (A.R. Siems-Anderson), zach.asher@wmich.edu (Z.D. Asher).

https://doi.org/10.1016/j.trip.2023.100766

Available online 22 February 2023
2590-1982/© 2023 The Author(s). Published by Elsevier Ltd. This is an open access article under the CC BY-NC-ND license (http://creativecommons.org/licenses/by-nc-nd/4.0/).

Nomenclature

ADAS	Advanced Driver
ADS	Assistance Systems
ADS	Autonomous Driving Systems
ML	Machine Learning
RGB	Red, Green, Blue
ODD	Operational Design Domain
DNN	Deep Neural Network
CNN	Convolutional Neural Network
LiDAR	Light Detection And Ranging
NCEI	National Center for Environmental Information
SWE	Snow-Water Equivalent
ANOVA	Analysis Of Variance
SD	Standard Deviation

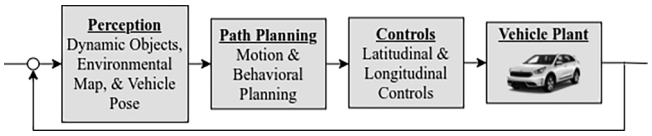

Fig. 1. Systems overview of a general vehicle automation system.

accumulation of snow (Neumeister et al., 2019). The use of LiDAR technology for lane detection in snow has been proposed by many researchers (Jung and Bae, 2018; Wang et al., 2019; Li et al., 2014; Shan et al., 2021; Li and Zhidong, 2013; Zhao and Yuan, 2012), but several have pointed out that, due to cost, compute requirements, and data degradation from snowfall, LiDAR is likely not a reliable solution in today's market (Rasshofer et al., 2011; Roy et al., 2020). To enable performance of these products in inclement weather, a method to algorithmically determine a category of inclement weather in real-time is needed so that purpose built perception techniques can be deployed.

This study provides the methods and evaluation techniques for development of snow-coverage estimation models which can be used in ADAS applications. Specifically, camera images and weather data are used as model inputs. There are a small number of papers with a similar scope that are worth reviewing in detail. Chronologically, the first study was conducted in 2011 by Jonsson who introduced a method for estimating the road weather conditions using a machine learning model trained with camera images and data from the Road Weather Information System (RWIS, see Pisano et al. (2007)) (Jonsson, 2011). This model was capable of achieving 91% accuracy on the given test set for classifying the road conditions into five different classes: dry, ice, snow, track, wet. Jonsson used Principal Component Analysis (PCA) to identify the key predictors used for model input, which showed to be a combination of image features and weather features. This model was lacking in that it used a limited amount of training data that was gathered from static images at intersections, and did not use on-road data for in-vehicle classification of road conditions. The second relevant series of studies from 2019 and 2021 present a direct application of ML techniques to detect snow from in-vehicle forward facing camera images (Khan and Ahmed, 2019; Khan et al., 2021). This work builds on traditional image processing, feature extraction, and classification (e.g., Bosch et al. (2007)) techniques to identify weather conditions from camera imagery with the use of machine learning (Haralick et al., 1973; Roser and Moosmann, 2008; Yan et al., 2009). Khan's results from 2019, which classified images into three levels of snowfall severity (clear, light snow, heavy snow) without weather data, yielded an accuracy of 95.9% using the Support Vector Machine (SVM) model with Local Binary Pattern (LBP) image features (Khan and Ahmed, 2019). However, the methods in this study focus on full image classification for snowfall, which may yield a different classification result than focusing on just the road surface needed for snow coverage estimation. Khan's results in 2021 yielded up to 91% accuracy in classifying images into multi-level weather conditions: clear, light rain, heavy rain, light snow, heavy snow, distant fog, near fog. But, since the model is focused on full image classification, it has not addressed the challenge for ADAS and ADS products needing to detect road infrastructure features. The methods and results of these studies are promising for providing vehicle-level weather conditions used mainly for object detection, however, the application of estimating snow coverage specifically on the road surface is not addressed in these studies. This research gap needs to be bridged to allow for eventual drivable region detection in snow from techniques such as tire track identification (Goberville et al., 2022).

To address the need for real-time road snow coverage estimation, this study proposes a combination of methods included from previous works. These methods include adding weather data into model development, recording and labelling a custom dataset, using ML models for classification, and varying different input feature sets to the ML models to achieve the highest accuracy classification of snow coverage. The high-level goal of this work is to provide a cost-effective technique for estimating snow coverage on the road's surface to achieve road-surface-level weather awareness to ADAS/ADS perception systems. This work provides specific details regarding custom camera data collection on snow-covered roads categorized as *none*, *standard*, or *heavy*, it provides insights on feature distributions in different snow coverage categories, and it shows the overall performance of various machine learning (ML) classification models for estimating the snow coverage.

1.1. Problem statement

Current ADS systems do not operate in inclement weather due to issues such as occluded lane lines. To solve this problem it is necessary both to develop quality datasets covering these road conditions and to develop a method to effectively identify inclement weather conditions.

2. Methodology

The methodology for this paper lays out the processes needed to successfully complete this research which is organized into these sections: image data collection, weather data acquisition, image data analysis, weather data analysis, and snow coverage estimation development.

2.1. Image data collection

The pipeline for image data collection contains the vehicle platform & sensors, route definition, data quality control and resampling, and subjective snow coverage assignment. Fig. 2 depicts this pipeline and each step is defined more in the following subsections.

2.1.1. Vehicle platform & sensors

The EEAV lab research vehicle platform was used for data collection in this research. This platform is built upon a 2019 Kia Niro containing a ZED 2 stereo camera, a Mobileye 630 (off-the-shelf computer vision), an Ouster LiDAR, a Delphi ESR radar, a FLIR thermal imaging camera, and two Swift Navigation Duro GPS antennas. For this research, only data from the Mobileye 630 and ZED 2 stereo camera were collected. The Mobileye 630 provided state-of-the-art lane line detections used to determine the performance of lane detection in snow and operated at 15 fps. The ZED 2 stereo camera provided raw RGB camera images used to build the dataset of snow-covered road images and operated at 30 fps.

2.1.2. Route & data quantity

The vehicle was driven during the 2020–2021 winter season in Kalamazoo, Michigan on a predefined route consisting of 5 different

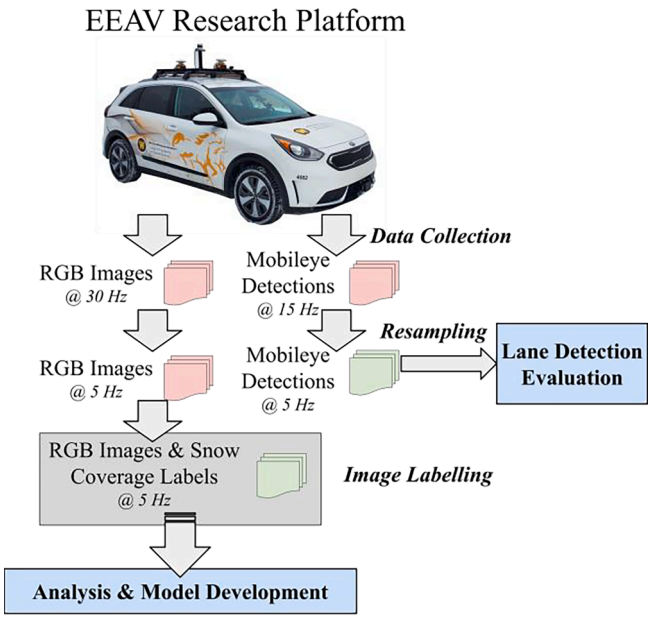

Fig. 2. Flowchart outlining the process used to prepare RGB images and CV system data for use in the analysis.

road sections as shown in Fig. 3. Each road section was selected based on having low traffic, two lanes, and clear, visible lane lines. After multiple weeks of data collection, there were over 1,500,000 frames of RGB images and Mobileye 630 lane detections recorded (Fig. 5).

2.1.3. Data resampling & quality control

The quantity of data was reduced after the videos and mobileye detections were resampled from 30 Hz and 15 Hz, respectively, to 5 Hz. The resampling was done to reduce the quantity of similar images used in analysis and to minimize overfitting during ML training. This resampling was followed by additional quality control assessments designed to eliminate extraneous variables (i.e., over-exposed images from glare, windshield wiper occlusion, poor resolution images from active precipitation, etc.), totaling the dataset to 21,375 images spanning 25 drive cycles. A route and date breakdown of these images is shown in Table 1.

2.1.4. Subjective snow coverage assignment

A subjective method was used for placing data from each road segment into one of three snow coverage categories: none, standard, or heavy. Each of the 25 videos from each road segment were used and assigned into one of these categories. Depending on how much snow was

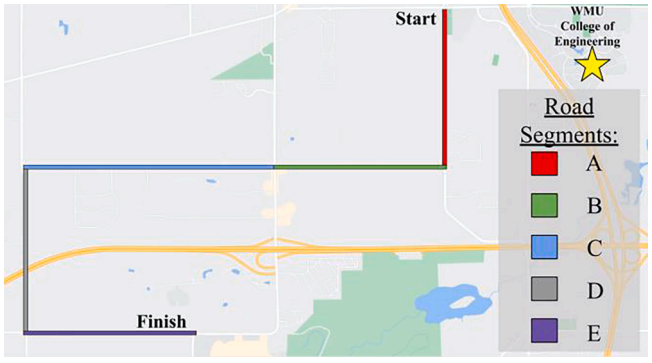

Fig. 3. Road segments used for data acquisition during the winter of 2020–2021 in Kalamazoo, MI. (Image acquired from google maps (Google maps., 2021) on 09/29/2021).

Fig. 5. General description of pixel-level, image-level, and video-level analysis including an example with images.

Table 1
Overview of the dataset collected consisting of RGB images. The road sections were assigned a letter per road section driven on. * Data from remaining road sections removed per quality control.

Date	Road Sections Included (see Fig. 3)	Road Segments	Total Images
01/18/2021	A, B*	2	1385
01/26/2021	A, B, C, D, E	6	5474
01/31/2021	A, B, C, D, E	6	5478
02/16/2021	A, B, C*	3	2828
02/18/2021	A, B, C, D, E	5	3730
02/19/2021	C, D, E*	3	2480
	Total	25	21375

covering the surface of the road during the entire road segment, all images within the video were labeled with the respective category. Fig. 4 shows examples of each image placed into each one of the categories mentioned along with the respective pixel histograms for each color channel. These histograms are used to extract features from each image that describe the snow coverage of the road. More will be discussed on the use of the histograms in section XXX..

The snow coverage labels were verified to be statistically significant by conducting a one-way ANOVA (Analysis of Variance) to determine the p-value for the relationship between the image-level RGB channel values and the snow coverage categories. As shown in Table 2, ANOVA provides insight in determining if there is statistical significance between the mean channel values and the groups of snow coverage that were determined for the labels. This significance indicates that there is variability in RGB values versus different levels of snow coverage. This correlation must be present if accurate machine learning or statistical models are to be developed for predicting snow coverage based on the mean and variance of RGB values (Table 3).

2.2. Image feature extraction

2.2.1. Region of interest

To eliminate the use of background pixels in the images, a static

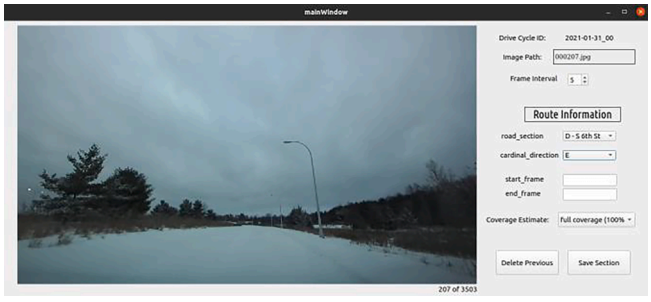

Fig. 4. Example images from each snow-coverage classification category with their corresponding RGB pixel histograms.

Table 2
ANOVA calculations which determine statistical significance between different levels of snow coverage.

w_0 = day of precipitation	w_1 = previous day precipitation
w_2 = 2 day average precipitation	w_3 = 2 day accumulation of precipitation
w_4 = 2 day average (including day of) precipitation	w_5 = 2 day accumulation (including day of) of precipitation

Table 3
ANOVA output showing strong statistical significance of snow coverage vs color channel mean pixel values.

Source	Sum of Squares	Degrees of Freedom	Mean Squares	F Value	p-value
		red channel vs snow coverage			
Between	8.57×10^6	2	4.29×10^6	25721.36	0.00
Within	3.56×10^6	21371	1.67×10^2	lightgray -	lightgray -
Total	1.21×10^7	21373	lightgray -	lightgray -	lightgray -
		green channel vs snow coverage			
Between	1.28×10^7	2	6.41×10^6	29467.74	yellow0.00
Within	4.65×10^6	21371	2.17×10^2	lightgray -	lightgray -
Total	1.75×10^7	21373	lightgray -	lightgray -	lightgray -
		blue channel vs snow coverage			
Between	1.25×10^7	2	6.26×10^6	31515.44	yellow0.00
Within	4.24×10^6	21373	1.98×10^2	lightgray -	lightgray -
Total	1.68×10^7	21373	lightgray -	lightgray -	lightgray -

region of interest (ROI) was used. The ROI mask was adjusted for a general fit of all images. This was possible because the road surfaces were all flat and the camera sensor was mounted in the same position for all road segments. A static ROI was used, allowing the road to be fully visible within the set ROI parameters for all images. From this ROI mask, the histograms of the RGB color channels were used for conducting the general analysis. Fig. 6 outlines the process masking images with the ROI mask and extracting RGB histograms for each image.

These histograms provide insight of pixel-value trends occurring in the image as a whole. To represent the image's RGB color channel distributions of pixel values, the mean and variances from each image's RGB histogram distribution were calculated for an image-level extraction of features as shown in Fig. 7. Then, to exploit video-level feature descriptions, these mean and variance values were averaged over the entire video segment (also shown in Fig. 10). Both the distributions of means and variances at the image level and the video level were used in the camera data analysis. These data are shown in the Results & Discussion.

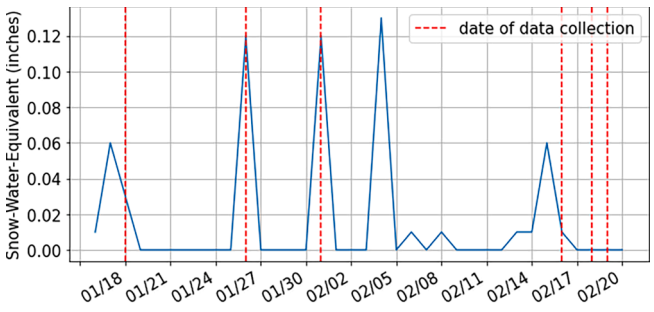

Fig. 6. Flow diagram of the process for extracting the ROI histograms from each video frame (or image).

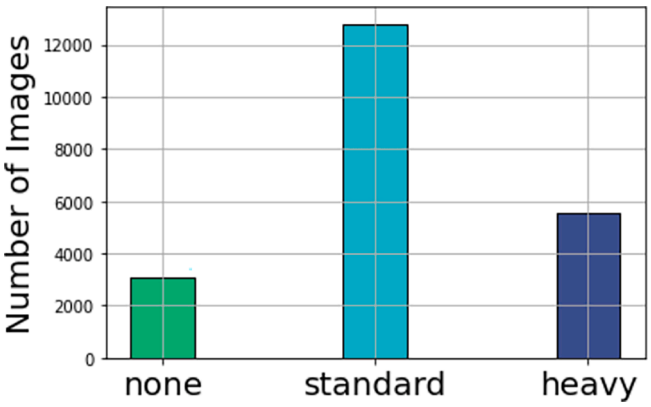

Fig. 7. Flow diagram outlining the process of exploiting video-level feature descriptions used for the final analysis.

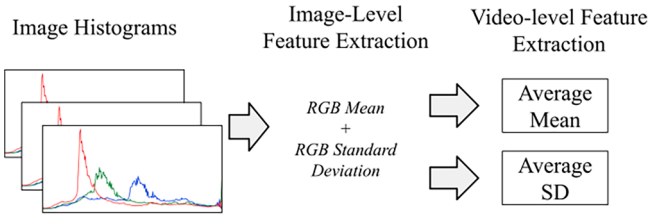

Fig. 10. Flow diagram outlining the process of exploiting video-level feature descriptions used for the final analysis.

2.3. Weather data analysis

The weather data included in this study was gathered from the National Center for Environmental Information (NCEI) database. The data used for this study came from the Kalamazoo/Battle Creek International Airport weather station, located approximately 7 miles from the data collection location (see Fig. 8 for a summary). This station records daily summaries of precipitation data. This daily precipitation metric is used to evaluate the snowfall via 6 different parameters.

The weather data parameters used for analysis are below:

2.4. Model development

Two different types of snow coverage estimation models were

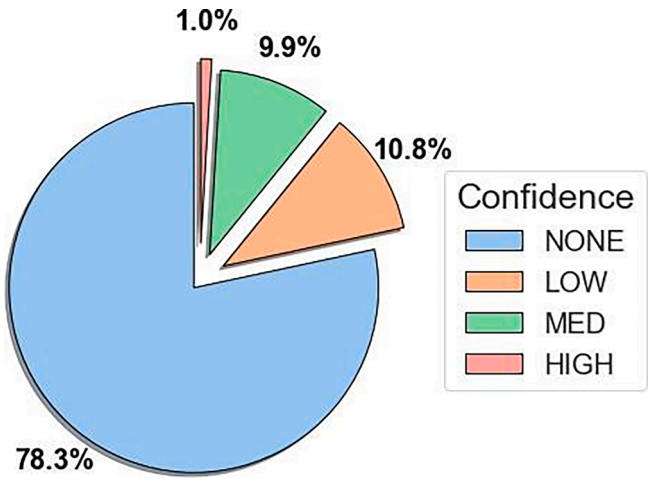

Fig. 8. Precipitation rates from 01/16/2021 to 02/20/2021 gathered from the Kalamazoo/Battle Creek International Airport land weather station. Data retrieved from noauthor2020-bu.

developed. The first uses image-level features to give an estimate of snow coverage at each frame. The second used video-level features to give an estimate of snow coverage along an entire segment of a road. The reason for this difference is the variation of temporal resolution of image data, video data, and weather data. Image data frequency is limited by the operational speed of the camera and image processing algorithms (FPS). Video data is limited on the number of images, *n*, included in a video segment. The weather data is limited on the frequency of available information from local weather stations. In this case, that frequency is daily. For the reason of very low weather resolution, video-level features were used in model development as the temporal resolution would be more similar to the resolution of weather data.

To build models for predicting the snow coverage on the road, the predictors placed as input to the model needed to be established. These predictors include both image predictors (e.g., mean RGB values) and weather predictors (e.g., previous day precipitation). It was important to understand the relationship with image data as well as weather data versus snow coverage in order to properly choose the necessary predictors for the model. Using the insights and analytical results established through the analysis of both camera and weather data, different ML models were trained. These models were trained using RGB mean and standard deviation for image-level features. The averages of these RGB mean and variance values within a video segment were used for video-level features. The weather feature used was the previous day precipitation as this was the weather parameter with the highest correlation to snow coverage (shown in Fig. reffigure13 in Results & Discussion).

The ML algorithm used was random forest as this provided the highest accuracy result when compared to others such as naive Bayes, logistic regression, K-nearest neighbor, support vector machines, and decision trees.

3. Methodology

In order to create an algorithm that successfully models snow coverage detection using camera data we first need to focus on camera data analysis and then on creation of a custom model. The dataset discussed in Section 2 was used for as the starting point for data analysis which requires a breakdown of image-level features, video-level features, and weather data. Creation of a custom snow coverage estimation model includes data labelling, ML algorithm set-up, and ML algorithm evaluations.

3.1. Data analysis

The custom dataset that was collected and used contains Mobileye lane detections, images organized into road segment videos, daily SWE values, and snow coverage labels. In order to use these data sources for estimating snow coverage, the image features and SWE accumulative metrics needed to be defined. The Mobileye data was used to evaluate the performance of state-of-the-art lane line detection in scenarios of snow coverage. Therefore, this data did not require any further feature extraction as it was not used in model development.

When compared to image frame rates (0.033–0.067 s per frame) and the video length in seconds per one mile road section (approximately 1.5 min average), snow surface accumulation changes on a much lower frequency, when snowfall is not currently present and the temperature remains below freezing (Datla and Sharma, 2010). With minimal fluctuations in surface temperature or snowfall, snow coverage on the roads surface can remain consistent for multiple hours (Kršmanc et al., 2013). When estimating the coverage of snow on a road's surface, this information can remain true as long as the snow on the road remains consistent. Because of this, two different snow coverage estimation models were developed for this study. One model estimates snow coverage given features from a single image (image-level estimation) to accommodate higher snow coverage variability. The other model will utilize video-level features for snow coverage estimation to accommodate lower snow coverage variability.

3.1.1. Image-level features

Images are a rich source of information containing pixel-level color channel values as well as spatial information since these pixel values are organized into a 3-dimensional array. Numerous image feature extraction methods exist for computer vision applications, however, since this research is meant to be foundational for snow coverage detection, it was decided to focus on RGB histograms as this has been shown to be used for accurate classification modelling (Mason and Duric, 2001). Additionally, the PCA conducted by Jonsson showed average histogram values were the variable with highest importance for weather estimation (Jonsson, 2011).

As the road surface is the focus for image feature extraction, the background of the images needed to be removed. To remove these background pixels, a static Region Of Interest (ROI) was used. The static ROI was chosen by selecting four points within the image that the road surface remains within for the entire dataset. Fig. 9 shows the flow diagram for how the histograms were extracted for each image using this ROI. These histograms show the distribution of pixel values contained within the road surface which was ultimately used for extracting key image features which can describe the snow coverage on the road surface.

In order to conduct image-to-image comparisons, the histogram for each color channel were converted to a normal distribution by calculating the mean (Eq. (1)) and standard deviation (SD) (Eq. (2)) of the pixel values as

$$\mu = \frac{1}{N}\sum_{i=1}^{N} x_i \tag{1}$$

$$SD = \sqrt{\frac{1}{N}\sum_{i=1}^{N}(x_i - \mu)^2} \tag{2}$$

where N is the total number of pixels in the ROI and x_i is each pixel value in the histogram. These mean and SD values were used as input to the ML models for estimating these conditions for image-level snow coverage estimation.

These features were combined into several different feature sets and used to train the ML models in this study. Each combination of features was used to train each ML model. The specific combinations used to train each of these models is shown in Table 4.

3.1.2. Video-level features

The video-level features were calculated by averaging the image-level means and SDs of all the images collected during a video segment. As an example, for a video segment containing 200 images, the mean and SD for each image was averaged using Eq. (1) to come up with a single value for the average video mean and the average video SD. These two average values are the features for video-level analysis and modelling. An overall conclusive diagram for this feature extraction methodology is shown in Fig. 7.

These features were combined into the same feature sets used in the image data set. And ML models were generated here as well. The specific combinations used to train each of these models is shown in the second

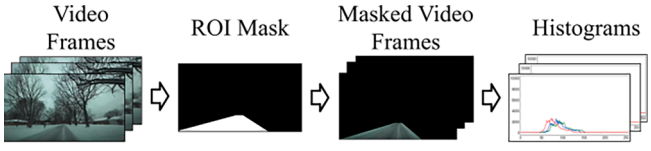

Fig. 9. Flow diagram of the process for extracting the ROI histograms from each image in a time-series video.

section of Table 4.

3.1.3. Daily SWE parameters

Accumulation of snow of the road surface is accounted for by including other parameters calculated based on daily SWE measurements (from Fig. 8). The different weather parameters and their descriptions are shown in the bullet list below. The correlation of these different parameters versus the snow coverage labels was done to determine which parameter best correlates with the snow coverage conditions. Ultimately, the value with the highest correlation was used in ML modelling for estimating the level of snow coverage.

- w_0 = day-of precipitation
- w_1 = previous day precipitation
- w_2 = 2-day average precipitation
- w_3 = 2-day total accumulation
- w_4 = 2-day average (including day-of) precipitation
- w_5 = 2-day total accumulation (including day-of)

3.2. Snow coverage estimation modeling

Two different models were developed to estimate the snow coverage on an image-level as well as a video-level. For training of both the image-level estimator and the video-level estimator, four different feature sets were used as an input. These feature sets are shown with the respective array shape for training and testing in Table 4.

3.2.1. Snow coverage labels

The subjective snow coverage labels discussed in Section 2.1.4 indicated as *none*, *standard*, or *heavy* were mapped to a unique integer for the purposes of training ML models for estimating the snow coverage condition. These three integer values were 0, 1, and 2, for *none*, *standard*, or *heavy* snow coverage, respectively. This mapping provided the representation of each snow coverage category in the ML training process.

3.2.2. ML algorithms

Six different ML algorithms were used to determine the algorithm/feature set pair with the best performance metrics. The ML algorithms evaluated were K-Nearest Neighbor (KNN), Naive-Bayes, Decision Trees, Random Forest, Logistic Regression, and Support Vector Machines (SVM) due to the capabilities of these algorithms for computing classification for computer vision applications (Sen et al., 2020; Osisanwo et al., 2017; Singh et al., 2016). All training scripts were written in python and the algorithms were accessed via the open-sourced "scikit-learn" python package.

3.2.3. Model evaluation

To accurately evaluate the models, the predicted outputs of the models were compared with the ground truth snow-coverage labels for evaluation on a test set (4275 image samples and five video samples). The potential metrics used were evaluated based on the ability to draw significant conclusions on the model performance (Sen et al., 2020). Accuracy was chosen to be used as the main model evaluation metric. It is calculated as

$$accuracy = \frac{CP}{TP} \tag{3}$$

where CP is the number of correct predictions and TP is the number of total predictions.

Table 4
Four different feature sets used for each model training.

Included Features	Train Array Shape	Test Array Shape
	Image-Level Estimation Feature Sets	
rgb-mean	(17,099,3)	(4275,3)
rgb-mean SWE precip	0.852(17,099,4)	0.852(4,275,4)
rgb-mean rgb-SD	0.852(17,099,6)	0.852(4,275,6)
rgb-mean rgb-SD SWE precip	0.852(17,099,7)	0.852(4,275,7)
	Video-Level Estimation Feature Sets	
rgb-mean	(20,3)	(5,3)
rgb-mean SWE precip	0.852(20,4)	0.852(5,4)
rgb-mean rgb-SD	0.852(20,6)	0.852(5,6)
rgb-mean rgb-SD SWE precip	0.852(20,7)	0.852(5,7)

4. Results & discussion

The results of this research include an overview of the analyses conducted for image-level, video-level, and weather data as well as the results of ML training for snow coverage estimation using both image-level features and video-level features with the varying feature sets as discussed in Section 3.1.

4.1. Image-level feature analysis

The mean and SD of red, green, and blue pixel values within the ROI of each image in the dataset were calculated and used for image-level features, as presented in Section 2.2.1. To show the distribution of mean values per snow coverage condition, violin plots were created for each color channel as shown in Fig. 11. From these plots, a few key insights can be made. First, all three color channels follow a similar distribution in which the mean pixel value for *none*, *standard*, or *heavy* snow continuously increases as the level of snow coverage increases

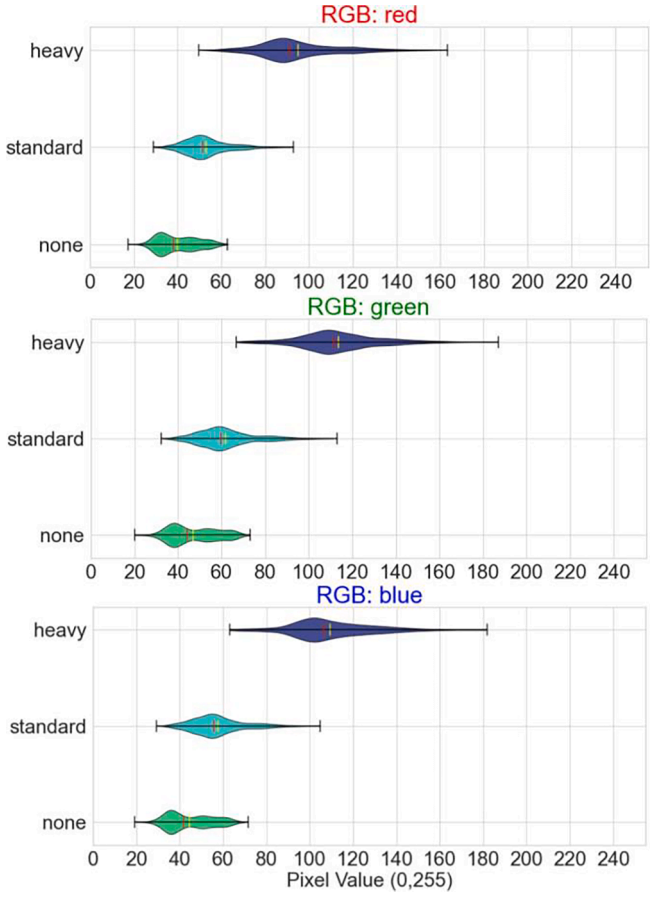

Fig. 11. Distribution of RGB color channel mean values for each snow coverage condition.

from *none* to *heavy*. The red color channel saw a 32.62% increase from *none* to *standard* and 79.48% increase from *standard* to *heavy* snow coverage. Green saw a 32.09% and 83.56% increase of these same differences, and blue saw a 29.45% and 89.82% increase. A second key observation is the type of distribution for each snow coverage condition. *Heavy* and *standard* snow coverages appear to follow very closely to a normal distribution, however, the *none* category has more mean values extending past the peak of the distribution. This could indicate there needs to be additional features to classify the *none* category more accurately, as there is higher variance in these mean pixel values. Overall, these diagrams show that there is certainly variance in the mean pixel values depending on the snow coverage on the road, allowing good indication of high accuracy using machine learning for estimation.

4.2. Video-level feature analysis

Similar to the image-level features, the video-level features are the average mean and average standard deviation of all the red, green, and blue pixel values within the ROI for all images in a video segment. By plotting the average mean values for each video segment in Fig. 12, the correlation of snow coverage versus video-level features could be made. From this plot, it can be seen that, similar to image-level, there is some overlap with the values in the none and standard coverage condition. However, including standard deviation (shown in Fig. 13) in the modelling allows for not only the mean value to be used to estimate snow coverage, but also the variation in the values is accounted for in the standard deviation. Another observation is the increase in values for the heavy snow coverage condition. Using just the mean value as a video-level feature, it could be possible to estimate snow coverage for the *heavy* condition. Lastly, similar to the image-level feature values, there is a continuous increase from *none* to *heavy* snow coverage. The *none* snow category yields an average value of 40.59, 47.64, 45.241 for red, green, and blue, respectively. *Standard* snow coverage yields 52.08, 60.64, 56.44, and *heavy* coverage yields 96.59, 115.38, 110.54 for red, green, and blue respectively. This finding demonstrates the capability of utilizing the video-level features for estimating snow coverage using ML.

4.3. Weather data feature analysis

The correlation of the weather data parameters described in Section 2.2.3 and the snow coverage labels given was observed via plotting the correlation heat map between these values, shown in Fig. 14. From this heat map, the most correlation is between w_1, w_2, & w_3 having average correlation values of 0.48, 0.467, and 0.467, respectively. All three of these parameters include the previous day's precipitation values. As most data collection was done early in the morning, the previous day's precipitation was expected to have the most impact on snow coverage on the road. Even though w_1, w_2, & w_3 have the highest correlation value within the other calculated weather parameters, correlations of under 0.5 are not typically viewed as high correlation. A key takeaway from this observation is that although these specific weather features are not highly correlated with the RGB images, there is reason to believe more effort should be placed in gathering higher fidelity temporal data. One potential cause of these correlation values is the temporal difference of the data. The images are recorded at 5 Hz, while the weather data is only recorded once per day. If weather data can be accessed at a higher frequency, there may be higher correlation with the RGB values than observed.

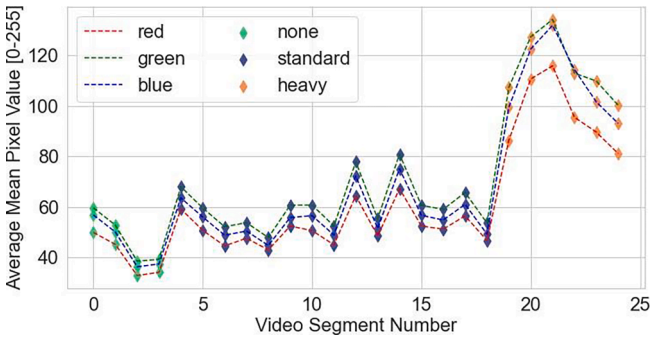

Fig. 12. Video-level average color channel values grouped into snow coverage labels.

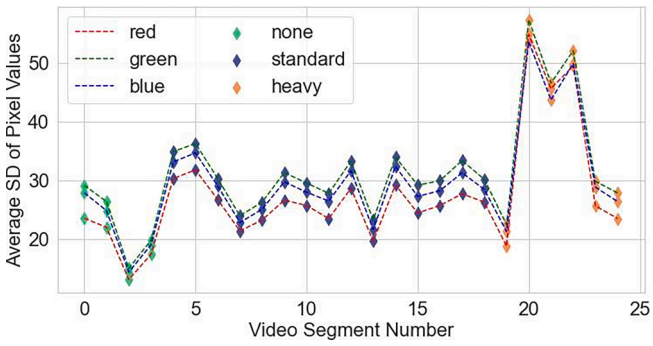

Fig. 13. Video-level standard deviation of pixel values grouped into snow coverage labels.

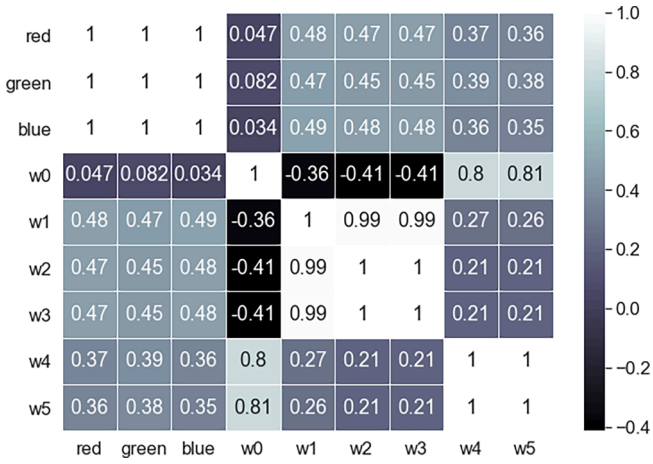

Fig. 14. Correlation heat map between RGB color channels and the weather metrics.

4.4. Evaluation of snow coverage estimation models

Results were obtained for a total of 48 different ML models. The image-level and video-level feature sets shown in Table 4 were used to train each ML model: K-Nearest Neighbor, Naive-Bayes, Decision Trees, Random Forest, Logistic Regression, and Support Vector Machines. The results of the image-level and video-level models are shown in Tables 5 and 6, respectively.

For image-level estimation, the order of best performance of ML algorithms was random forest, KNN, decision trees, support vector machines, logistic regression, and then Naive-Bayes. For the variation in feature sets used as input to the model, the feature set including RGB mean, RGB standard deviation, and the w_1 weather feature performed the best for each ML algorithm. This shows that including weather data along with the mean and standard deviation in image data yields the highest accuracy model for estimating snow coverage, no matter what algorithm is used. The overall highest performing model that achieved 95.63% accuracy is the random forest model trained with RGB mean, RGB standard deviation, and the w_1 weather feature.

The video-level estimation models were only trained with twenty

Table 5
Model accuracy results for image-level snow estimation (No. train samples = 17,099; No. test samples = 4,275). The yellow–highlighted cell indicates the model and feature set combination with the highest accuracy. The boldfaced values indicate the highest performing feature set on the specific ML algorithm.

Features	SVM	DT	RF	Naive-Bayes	KNN	Logistic
rgb-mean	0.8795	0.8760	0.9142	0.7890	0.9127	0.8414
rgb-mean & SWE	0.8763	0.8926	0.9228	0.8108	0.9120	0.82707
rgb-mean & rgb-std	0.8996	0.9256	0.9485	0.8084	0.9506	0.8508
rgb-mean, rgb-std, & SWE	0.9036	0.9401	0.9563	0.8271	0.9516	0.8501

Table 6
Model accuracy results for video-level snow estimation (No. train samples = 20; No. test samples = 5). The boldfaced values indicate the highest performing feature set on the specific ML algorithm.

Features	SVM	DT	RF	Naive-Bayes	KNN	Logistic
rgb-mean	0.8	0.8	**1.0**	0.8	0.8	**1.0**
rgb-mean & SWE	0.8	**1.0**	**1.0**	**1.0**	0.6	**1.0**
rgb-mean & rgb-std	0.8	0.6	0.8	**1.0**	0.6	**1.0**
rgb-mean, rgb-std, & SWE	0.8	0.6	0.8	0.6	0.8	0.6

samples and tested with five. Although the size of this dataset could be improved, there are still meaningful conclusions that can be drawn regarding the best feature set and ML algorithm for yielding the highest accuracy for snow estimation using video-level features. From Table 6, it can be seen that the inputs of RGB mean and SWE are best because four of six models using that feature set was able to accurately estimate the snow coverage in the five test cases. This is a different feature set that yielded the best results for image-level estimation.

4.5. Future work

The dataset developed here provides significant possibilities for additional research. Continuing work to expand the dataset can help address the need for additional inclement weather driving data. This dataset will help enable development of future ADS and ADAS systems designed to better handle these inclement weather conditions.

Deep learning models such as a Convolutional Neural Network (CNN), which historically excels in image classification tasks (Kumar et al., 2020), can be trained using this dataset to potentially provide more accurate weather classification. These CNNs could also be developed to perform finer classification of road conditions, providing more levels of snow coverage than the three used in this paper. Additional labelling to identify various common types of occlusion such as glare could also have useful applications.

This dataset also provides an excellent opportunity to develop custom deep learning solutions to common ADS tasks such as lane keeping. A deep learning technique such as a CNN could be trained to accurately identify the position of lane lines even when they are occluded by snow.

5. Conclusions

In this study, a custom dataset composed of raw camera images, commercial off the shelf state-of-the-art lane line detections, and weather data from local airport weather stations was collected in Kalamazoo, Michigan during the 2020–2021 winter season. This dataset was then used for observing the statistical significance of image-level features, video-level features, and weather precipitation values for on-road snow coverage. Upon seeing correlation with the features versus snow coverage conditions, six different machine learning algorithms were trained and tested using various combinations of features to estimate snow coverage on an image-level and video-level, individually. The image-level model achieved 95.63% accuracy on the test set using the RGB mean, RGB standard deviation, and the previous day precipitation values trained on a random forest model. The video-level estimator achieved complete accuracy for a three-option categorization tested on five samples.

Snow coverage estimation using on-vehicle sensors enables ADAS and ADS products to begin approaching the operation in snow problem. Expanding the ODD through operation in snow is a critical problem for offsetting annual fatalities and accidents, as the current ADAS systems need to disengage when low confident detections are present. This is not a problem that can be fixed by simply throwing more training data at a deep neural network and researchers need to start developing more foundational solutions now (Lee et al., 2021). This work provides foundational research to enable hierarchical ADAS and ADS operation for different weather types. This work can be expanded by utilizing more detailed image features for snow coverage estimation and increased temporal resolution of weather data. This can be achieved by utilizing weather sensors installed directly onto a research vehicle platform. Once weather scenarios can be reliably detected, autonomous driving on snow-covered road conditions can be achieved, thus, minimizing 1.32 million annual accidents saving potentially over 6,000 lives per year.

CRediT authorship contribution statement

Nicholas A. Goberville: Methodology, Software, Formal analysis, Investigation, Data curation, Writing – original draft, Visualization, Supervision. **Kyle R. Prins:** Writing – review & editing, Visualization. **Parth Kadav:** Software, Writing – review & editing. **Curtis L. Walker:** Writing – review & editing, Resources, Conceptualization. **Amanda R. Siems-Anderson:** Writing – review & editing, Resources, Conceptualization. **Zachary D. Asher:** Supervision, Project administration, Funding acquisition, Conceptualization.

Declaration of Competing Interest

The authors declare the following financial interests/personal relationships which may be considered as potential competing interests: Nicholas A Goberville reports a relationship with Revision Autonomy LLC that includes: equity or stocks. Zachary D. Asher reports a relationship with Revision Autonomy LLC that includes: board membership, employment, and equity or stocks.

Acknowledgment

NCAR coauthor contributions are based upon work supported by the National Center for Atmospheric Research, which is a major facility sponsored by the National Science Foundation under Cooperative Agreement No. 1852977. Any opinions, findings and conclusions or recommendations expressed in this material do not necessarily reflect the views of the National Science Foundation.

References

Bosch, A., Zisserman, A., and Munoz, X., 2007. Image classification using random forests and ferns. In 2007 IEEE 11th International Conference on Computer Vision, pp. 1–8.

Datla, S., and Sharma, S., 2010. Variation of impact of cold temperature and snowfall and their interaction on traffic volume. Transp. Res. Rec., 2169(1), Jan., pp. 107–115.

European New Car Assessment Program, 2019. TEST PROTOCOL – lane support systems. Tech. Rep. Version 3.0.2, European New Car Assessment Program, July.

Flannagan, C., LeBlanc, D., Bogard, S., Nobukawa, K., Narayanaswamy, P., Leslie, A., Raymond, K., Beck, C., Marchione, Lobes, K., 2016. Large-Scale field test of forward collision alert and lane departure warning systems. National Highway Traffic Safety Administration. Tech. Rep. DOT HS 812 247.

Goberville, N., El-Yabroudi, M., Omwanas, M., Rojas, J., Meyer, R., Asher, Z.D., Abdel-Qader, I., 2020. Analysis of LiDAR and camera data in Real-World weather conditions for autonomous vehicle operations. SAE Int. J. Adv. Curr. Practices Mobility. V129-99EJ.

Goberville, N.A., Kadav, P., and Asher, Z.D., 2022. Tire track identification: A method for drivable region detection in conditions of snow-occluded lane lines. In SAE Technical Paper Series, no. 2022–01-0083, SAE International.

Google maps.https://www.google.com/maps/- @42.2674432,-85.6260608,14z. Accessed: 2021-10-19.

Haralick, R.M., Shanmugam, K., Dinstein, I., 1973. Textural features for image classification. IEEE Trans. Syst. Man Cybern. SMC-3, 610–621.

Insurance Institute for Highway Safety, 2020. Real-world benefits of crash avoidance technologies. Tech. rep., Insurance Institute for Highway Safety & Highway Loss Data Institute, Dec.

Jonsson, P., 2011. Classification of road conditions: From camera images and weather data. In 2011 IEEE International Conference on Computational Intelligence for Measurement Systems and Applications (CIMSA) Proceedings, pp. 1–6.

Jung, J., Bae, S.-H., 2018. Real-Time road lane detection in urban areas using LiDAR data. Electronics 7 (11), 276.

Khan, M.N., Ahmed, M.M., 2019. Snow detection using In-Vehicle video camera with Texture-Based image features utilizing K-Nearest neighbor, support vector machine, and random forest. Transp. Res. Rec. 2673 (8), 221–232.

Khan, M.N., Das, A., Ahmed, M.M., Wulff, S.S., 2021. Multilevel weather detection based on images: a machine learning approach with histogram of oriented gradient and local binary pattern-based features. J. Intell. Transp. Syst. 25 (5), 513–532.

Kršmanc, R., Slak, A. Š., and Demšar, J., 2013. Statistical approach for forecasting road surface temperature. Meteorol. Appl. 20(4), pp. 439–446.

Kumar, N., Kaur, N., and Gupta, D., 2020. Major convolutional neural networks in image classification: A survey. In Proceedings of International Conference on IoT Inclusive Life (ICIIL 2019), NITTTR Chandigarh, India, Lecture Notes in Networks and Systems. Springer Singapore, Singapore, Apr., pp. 243–258.

Lee, Y., Jeon, J., Ko, Y., Jeon, B., Jeon, M., 2021. Task-Driven deep image enhancement network for autonomous driving in bad weather. In 2021 IEEE International Conference on Robotics and Automation (ICRA), ieeexplore.ieee.org. pp. 13746–13753.

Li, T., and Zhidong, D., 2013. A new 3D LIDAR-based lane markings recognition approach. In 2013 IEEE International Conference on Robotics and Biomimetics (ROBIO), ieeexplore.ieee.org, pp. 2197–2202.

Li, Q., Chen, L., Li, M., Shaw, S.-L., Nüchter, A., 2014. A Sensor-Fusion Drivable-Region and Lane-Detection system for autonomous vehicle navigation in challenging road scenarios. IEEE Trans. Veh. Technol. 63 (2), 540–555.

Mason, M., Duric, Z., 2001. Using histograms to detect and track objects in color video. In Proceedings 30th Applied Imagery Pattern Recognition Workshop (AIPR 2001). Analysis and Understanding of Time Varying Imagery, ieeexplore.ieee.org, pp. 154–159.

National Highway and Traffic Safety Administration, 2018. Functional safety assessment of an automated lane centering system. Tech. Rep. DOT HS 812 573, U.S. Department of Transportation, Aug.

Neumeister, D.M., Pape, D.B., and Battelle Memorial Institute, 2019. Automated vehicles and adverse weather: Final report. Tech. Rep. FHWA-JPO-19-755, June.

Osisanwo, F.Y., Akinsola, J.E.T., Awodele, O., Hinmikaiye, J.O., Olakanmi, O., Akinjobi, J., 2017. Supervised machine learning algorithms: classification and comparison. Int. J. Comput. Trends Technol. 48 (3), 128–138.

Pisano, P.A., Pol, J.S., Stern, A.D., Boyce, B.C., and Garrett, J.K., 2007. Evolution of the US department of transportation clarus initiative: Project status and future plans. In Preprints, 23rd Conf. on Interactive Systems (IIPS) for Meteorology, Oceanography, and Hydrology, San Antonio, TX, Amer. Meteor. Soc. A, Vol. 4, ams.confex.com.

Rasshofer, R.H., Spies, M., Spies, H., 2011. "Influences of weather phenomena on automotive laser radar systems". Advances. Radio Sci. 9 (B. 2), 49–60.

Roser, M., and Moosmann, F., 2008. Classification of weather situations on single color images. In 2008 IEEE Intelligent Vehicles Symposium, pp. 798–803.

Roy, G., Cao, X., Bernier, R., Tremblay, G., 2020. Physical model of snow precipitation interaction with a 3D lidar scanner. Appl. Opt. 59 (25), 7660–7669.

Sen, P.C., Hajra, M., and Ghosh, M., 2020. Supervised classification algorithms in machine learning: A survey and review. In Emerging Technology in Modelling and Graphics, Springer Singapore, pp. 99–111.

Shan, Y., Yao, X., Lin, H., Zou, X., Huang, K., 2021. Lidar-Based stable navigable region detection for unmanned surface vehicles. IEEE Trans. Instrum. Meas. 70, 1–13.

Singh, A., Thakur, N., and Sharma, A., 2016. A review of supervised machine learning algorithms. In 2016 3rd International Conference on Computing for Sustainable Global Development (INDIACom), ieeexplore.ieee.org, pp. 1310–1315.

Society of Automotive Engineers, 2021. Taxonomy and definitions for terms related to driving automation systems for On-Road motor vehicles. Tech. Rep. J3016_202104, Apr.

Thorn, Eric, Kimmel, Shawn, 2018. A framework for automated driving system testable cases and scenarios. National Highway Traffic Safety Administration. Tech. Rep. DOT HS 812 623.

Vargas, J., Alsweiss, S., Toker, O., Razdan, R., and Santos, J., 2021. An overview of autonomous vehicles sensors and their vulnerability to weather conditions. Sensors 21(16).

Walker, C.L., Boyce, B., Albrecht, C.P., Siems-Anderson, A., 2020. Will weather dampen Self-Driving vehicles? Bull. Am. Meteorol. Soc. 101 (11), E1914–E1923.

Wang, Z., Zeng, C., Yang, X.U., Luo, J., and Hu, J., 2019. Real-time drivable region planning based on 3D LiDAR. DEStech Transactions on Computer Science and Engineering, 0(cisnrc).

Yan, X., Luo, Y., Zheng, X., 2009. Weather recognition based on images captured by vision system in vehicle. In: Advances in Neural Networks – ISNN 2009. Springer, Berlin Heidelberg, pp. 390–398.

Zhao, G., and Yuan, J., 2012. Curb detection and tracking using 3D-LIDAR scanner. In 2012 19th IEEE International Conference on Image Processing, ieeexplore.ieee.org, pp. 437–440.